

Green's Function Approach to Inclusive Electron Scattering *

F. Capuzzi, C. Giusti, A. Meucci and F.D. Pacati

Dipartimento di Fisica Nucleare e Teorica, Università degli Studi di Pavia, and
Istituto Nazionale di Fisica Nucleare, Sezione di Pavia, Pavia, Italy

Abstract

A Green's function approach to the inclusive quasielastic (e, e') scattering is presented. The components of the nuclear response are written in terms of the single-particle optical model Green's function. The explicit calculation of the Green's function can be avoided by its spectral representation, which is based on a biorthogonal expansion in terms of the eigenfunctions of the non-Hermitian optical potential and of its Hermitian conjugate. This allows one to treat final state interactions consistently in the inclusive (e, e') and in the exclusive $(e, e'N)$ reactions. Numerical results for the longitudinal and transverse response functions obtained in a nonrelativistic and in a relativistic framework are presented and discussed also in comparison with data.

1 Introduction

Inelastic electron scattering has proven to be a very precise tool for studying the excitation spectrum of atomic nuclei owing to the possibility of simultaneously varying energy and momentum transfer (ω, \mathbf{q}) [1]. In a representation of the nuclear response as a function of ω and q a large broad peak occurs at about $\omega = q^2/2M$. Its position corresponds to the elastic peak in electron scattering by a free nucleon. It is quite natural to assume that a quasifree process is responsible for such a peak with a nucleon emitted quasielastically. Coincidence $(e, e'N)$ experiments in the quasifree region confirm such a picture and represent a valuable source of information on single-nucleon degrees of freedom inside nuclei.

In the inclusive (e, e') process only the scattered electron is detected and the final nuclear state is undetermined, but the main contribution in the region of the quasielastic (QE) peak comes from the interaction on single nucleons. If the nucleons were indeed free, the peak would be sharp and would just occur at the energy loss $\omega = q^2/2M$ corresponding to the energy taken by the recoiling free nucleon. A shift in the position of the peak is produced by the nuclear binding,

*presented by C. Giusti, E-mail: giusti@pv.infn.it, phone: +39 0382507454, fax: +39 0382526938.

while a broadening of the peak is produced by Fermi motion. A very simple model, where the cross section is given by the interaction on all the constituent nucleons of the nucleus and a Fermi gas model is assumed for nuclear structure, is indeed able to give a remarkably good description of the cross section in the QE region [2]. This same model, however, is not able to describe simultaneously the QE longitudinal and transverse responses, whose Rosenbluth separation has been experimentally achieved on a variety of nuclei and over a large range of momentum transfers [1].

In the one-photon exchange approximation and assuming the plane-wave approximation for the incident and the outgoing electrons, the (e, e') cross section is given by [1]

$$\sigma_{\text{inc}} = K (2\varepsilon_L R_L + R_T) , \quad (1)$$

where K is a kinematical factor and

$$\varepsilon_L = \frac{Q^2}{q^2} \left(1 + 2 \frac{q^2}{Q^2} \tan^2 (\vartheta_e/2) \right)^{-1} \quad (2)$$

measures the polarization of the virtual photon. In Eq. (2) ϑ_e is the scattering angle of the electron, $Q^2 = \mathbf{q}^2 - \omega^2$, and $q^\mu = (\omega, \mathbf{q})$ is the four momentum transfer. The longitudinal and transverse response functions, R_L and R_T are defined by

$$R_L(\omega, q) = W_{\text{tot}}^{00}(\omega, q), R_T(\omega, q) = W_{\text{tot}}^{xx}(\omega, q) + W_{\text{tot}}^{yy}(\omega, q) , \quad (3)$$

in terms of the diagonal components of the hadron tensor

$$W_{\text{tot}}^{\mu\mu}(\omega, q) = \int \sum_f | \langle \Psi_f | J^\mu(\mathbf{q}) | \Psi_0 \rangle |^2 \delta(E_0 + \omega - E_f) . \quad (4)$$

Here J^μ is the nuclear charge-current operator which connects the initial state $|\Psi_0\rangle$ of the nucleus, of energy E_0 , with the final states $|\Psi_f\rangle$, of energy E_f . In the inclusive (e, e') process the sum is over a complete set of final nuclear states and only the diagonal components of the hadron tensor contribute, while in the exclusive $(e, e'N)$ process also the nondiagonal components contribute and the cross section is in general given in terms of a larger number of structure functions [1].

The separation of the response functions R_L and R_T can experimentally be achieved from Eq. (1) by varying electron kinematics. In a plot of the cross section as function ε_L , for fixed values of ω and Q^2 , the slope gives R_L and the extrapolated intercept with the vertical axis at $\varepsilon_L = 0$ gives R_T . Such a Rosenbluth separation [3] has been achieved in the 80's and 90's on different nuclei [1].

A huge amount of theoretical work was produced over the past two decades in order to explain the problem raised by the experimental separation of R_L and R_T [1]. The main problem was the apparent quenching of R_L , while for R_T there is in general an apparent excess of strength. Different approaches, with different theoretical ingredients, obtained partial success in explaining either the longitudinal or the transverse response, but despite all these efforts some problems are still open and a consistent and simultaneous description of R_L and R_T data has not

been achieved. Some confusion is also due to the experimental situation. These experiments of separation are difficult and data from different laboratories are sometimes in disagreement. New experiments with improved experimental accuracy would be helpful to make the experimental situation clearer. New measurements are planned at Jlab [4]

In this contribution we present a Green's function approach to the inclusive QE (e, e') scattering. With our work we don't aim at a unified and consistent description of R_L and R_T data. The model contains approximations. It is basically a single-particle approach, where only the one-body part of the nuclear current is retained. Calculations of two-body contributions performed by different groups have given different results [1, 5]. There are, however, consistent indications that the combined effect of two-body current and tensor correlations can be appreciable on the transverse response [6, 7, 5]. Thus, with our model we don't expect to describe R_T data, while the main contributions to R_L should already be included. Our aim is to study the effects of final state interactions (FSI). FSI are an important ingredient of the inclusive electron scattering, since they are essential to explain the exclusive one-nucleon emission, which gives the main contribution to the inclusive reaction in the QE region. The absorption in a given final state due, e.g., to the imaginary part of the optical potential, produces a loss of flux that is appropriate for the exclusive process, but inconsistent for the inclusive one, where all the allowed final channels contribute and the total flux must be conserved.

This conservation is preserved in the Green's function approach, where the components of the nuclear response are written in terms of the single-particle optical model Green's function. This result was originally derived by arguments based on the multiple scattering theory [8] and successively by means of the Feshbach projection operator formalism [9, 10, 11, 12]. The spectral representation of the single-particle Green's function, based on a biorthogonal expansion in terms of the eigenfunctions of the non-Hermitian optical potential, allows one to perform explicit calculations and to treat FSI consistently in the inclusive and in the exclusive reactions. Important and peculiar effects are given, in the inclusive reactions, by the imaginary part of the optical potential, which is responsible for the redistribution of the strength among different channels. The approach has been developed and used in a nonrelativistic frame [11] and, more recently, also in a relativistic frame [13]. Although some differences and complications are due to the Dirac matrix structure, the formalism follows in both frames the same steps and approximations. The numerical results obtained in both frames allow us to check the relevance of relativistic effects.

The Green's function approach is presented in Sec. 2. In Sec. 3 some results for R_L and R_T are presented and discussed also in comparison with data. Summary and conclusions are drawn in Sec. 4.

2 The Green's function approach

The response functions of the inclusive (e, e') scattering are defined in Eq. (3) in terms of the diagonal components of the hadron tensor of Eq. (4), that can equivalently be expressed as

$$W_{\text{tot}}^{\mu\mu}(\omega, q) = -\frac{1}{\pi} \text{Im} \langle \Psi_0 | J^{\mu\dagger}(\mathbf{q}) G(E_f) J^\mu(\mathbf{q}) | \Psi_0 \rangle , \quad (5)$$

where $E_f = E_0 + \omega$ and $G(E_f)$ is the Green's function related to the nuclear Hamiltonian H , i.e.,

$$G(E_f) = \frac{1}{E_f - H + i\eta} . \quad (6)$$

Here and in all the equations involving G the limit for $\eta \rightarrow +0$ is understood. It must be performed after calculating the matrix elements between normalizable states.

The hadronic tensor in Eq. (5) contains the full $(A+1)$ -body propagator of the nuclear system and, as such, it is an extremely complicated object, which defies a practical evaluation. Only an approximated treatment reduces the problem to a tractable form. Under suitable approximations the nuclear response can be written in terms of the optical-model Green's function [11].

The first approximation consists in retaining only the one-body part of the charge-current operator J^μ . Thus, we set

$$J^\mu(\mathbf{q}) = \sum_{i=1}^{A+1} j_i^\mu(\mathbf{q}) , \quad (7)$$

where j_i^μ acts only on the variables of the nucleon i . By Eq.(7), one can express the hadron tensor as the sum of two terms, i.e.,

$$W_{\text{tot}}^{\mu\mu}(\omega, q) = W^{\mu\mu}(\omega, q) + W_{\text{coh}}^{\mu\mu}(\omega, q) , \quad (8)$$

where $W^{\mu\mu}(\omega, q)$ is the incoherent hadron tensor [14], which contains only the diagonal contributions $j_i^{\mu\dagger} G j_i^\mu$, whereas the coherent hadron tensor $W_{\text{coh}}^{\mu\mu}(\omega, q)$ gathers the residual terms of interference between different nucleons. As the incoherent hadron tensor, also $W_{\text{coh}}^{\mu\mu}(\omega, q)$ can be expressed in terms of single-particle quantities (see Sect. 9 of Ref. [12]), but for the transferred momenta considered here we can take advantage of the high- q approximation [15] and retain only $W^{\mu\mu}(\omega, q)$. This term can be further simplified using the symmetry of G for the exchange of nucleons and the antisymmetrization of $|\Psi_0\rangle$. Therefore, we write

$$W_{\text{tot}}^{\mu\mu}(\omega, q) \simeq W^{\mu\mu}(\omega, q) = -\frac{A+1}{\pi} \text{Im} \langle \Psi_0 | j^{\mu\dagger}(\mathbf{q}) G(E_f) j^\mu(\mathbf{q}) | \Psi_0 \rangle , \quad (9)$$

where $j^\mu(\mathbf{q})$ is the component of $J^\mu(\mathbf{q})$ related to an arbitrarily selected nucleon.

Let $|n\rangle$ and $|\varepsilon\rangle$ denote the eigenvectors of the residual Hamiltonian H_R of A interacting nucleons related to the discrete and continuous eigenvalues ε_n and ε ,

respectively. We introduce the operators P_n , projecting onto the n -channel subspace of \mathcal{H} , and Q_n , projecting onto the orthogonal complementary subspace, i.e.,

$$P_n = \int d\mathbf{r} |\mathbf{r}; n\rangle \langle n; \mathbf{r}|, \quad Q_n = 1 - P_n. \quad (10)$$

Here $|\mathbf{r}; n\rangle$ is the vector obtained from the tensor product between the discrete eigenstate $|n\rangle$ of H_R , and the orthonormalized eigenvectors $|\mathbf{r}\rangle$ of the selected nucleon. Moreover, we introduce the projection operator onto the continuous channel subspace, i.e.,

$$P_c = \int d\varepsilon \int d\mathbf{r} |\mathbf{r}; \varepsilon\rangle \langle \varepsilon; \mathbf{r}|. \quad (11)$$

Due to the completeness of the set $\{|\mathbf{r}; n\rangle, |\mathbf{r}; \varepsilon\rangle\}$, one has

$$\sum_n P_n + P_c = 1. \quad (12)$$

Then, we insert Eq. (12) into Eq. (9) disregarding the contribution of P_c . This approximation, which simplifies the calculations, is correct for sufficiently high values of the transferred momentum q . Thus, the hadron tensor of Eq. (9) can be expressed as the sum

$$W^{\mu\mu}(\omega, q) = W_d^{\mu\mu}(\omega, q) + W_{\text{int}}^{\mu\mu}(\omega, q), \quad (13)$$

of a direct term

$$\begin{aligned} W_d^{\mu\mu}(\omega, q) &= \sum_n W_n^{\mu\mu}(\omega, q), \\ W_n^{\mu\mu}(\omega, q) &= -\frac{A+1}{\pi} \text{Im} \langle \Psi_0 | j^{\mu\dagger}(\mathbf{q}) P_n G(E_f) P_n j^\mu(\mathbf{q}) | \Psi_0 \rangle, \end{aligned} \quad (14)$$

and of a term

$$\begin{aligned} W_{\text{int}}^{\mu\mu}(\omega, q) &= \sum_n \widehat{W}_n^{\mu\mu}(\omega, q), \\ \widehat{W}_n^{\mu\mu}(\omega, q) &= -\frac{A+1}{\pi} \text{Im} \langle \Psi_0 | j^{\mu\dagger}(\mathbf{q}) P_n G(E_f) Q_n j^\mu(\mathbf{q}) | \Psi_0 \rangle, \end{aligned} \quad (15)$$

which gathers the contributions due to the interference between the intermediate states $|\mathbf{r}; n\rangle$ related to different channels.

If we disregard the effects of interference between different channels and consider only the direct contribution to the hadron tensor of Eq. (14), the matrix elements of $P_n G(E) P_n$ in the basis $|\mathbf{r}; n\rangle$ define the single-particle Green's function $\mathcal{G}_n(E)$ [11] of the single-particle Feshbach optical potential $\mathcal{V}_n(E)$ [17]

$$\mathcal{G}_n(E) = \frac{1}{E - T - \mathcal{V}_n(E) + i\eta}, \quad (16)$$

which describes the elastic scattering of a nucleon by an A-nucleus in the discrete state $|n\rangle$. Using the definition of P_n in Eq. (10), the direct hadron tensor $W_n^{\mu\mu}(\omega, q)$ of Eq. (14) can be reduced to the single-particle expression

$$W_n^{\mu\mu}(\omega, q) = -\frac{1}{\pi} \lambda_n \text{Im} \langle \varphi_n | j^{\mu\dagger}(\mathbf{q}) \mathcal{G}_n(E_f - \varepsilon_n) j^\mu(\mathbf{q}) | \varphi_n \rangle , \quad (17)$$

where λ_n is the spectral strength [16] of the hole state φ_n , which is the normalized overlap integral between $|\Psi_0\rangle$ and $|n\rangle$. The problem of expressing the interference hadron tensor $\widehat{W}_n^{\mu\mu}$ in a one-body form is treated in Ref. [11]. It is argued that the contribution of $\widehat{W}_n^{\mu\mu}$ can be included into the direct hadron tensor $W_n^{\mu\mu}$ by the simple replacement

$$\mathcal{G}_n(E) \rightarrow \mathcal{G}_n^{\text{eff}}(E) \equiv \sqrt{1 - \mathcal{V}'_n(E)} \mathcal{G}_n(E) \sqrt{1 - \mathcal{V}'_n(E)} , \quad (18)$$

where $\mathcal{V}'_n(E)$ is the energy derivative of the Feshbach optical potential.

In principle, different optical potentials \mathcal{V}_n must be considered for different values of n . As neither microscopic nor empirical calculations are available for the optical potential \mathcal{V}_n associated with the excited states, a common practice relates them to the ground state potential \mathcal{V}_0 by means of an appropriate energy shift. Therefore we set

$$\mathcal{V}_n(E) \simeq \mathcal{V}_0(E) , \quad (19)$$

which implies

$$\mathcal{G}_n(E) \simeq \mathcal{G}_0(E) . \quad (20)$$

Using these approximations, we write

$$W^{\mu\mu}(\omega, q) = -\frac{1}{\pi} \sum_n \lambda_n \text{Im} \langle \varphi_n | j^{\mu\dagger}(\mathbf{q}) \mathcal{G}_0^{\text{eff}}(E_f - \varepsilon_n) j^\mu(\mathbf{q}) | \varphi_n \rangle . \quad (21)$$

As a next step, the spectral representation of the single-particle Green's function function can be used in order to allow practical calculations of the hadron tensor of Eq. (21).

In expanded form, the hadron tensor reads

$$\begin{aligned} W^{\mu\mu}(\omega, q) = & - \frac{1}{\pi} \sum_n \lambda_n \text{Im} \langle \varphi_n | j^{\mu\dagger}(\mathbf{q}) \sqrt{1 - \mathcal{V}'(E)} \\ & \times \mathcal{G}(E) \sqrt{1 - \mathcal{V}'(E)} j^\mu(\mathbf{q}) | \varphi_n \rangle , \end{aligned} \quad (22)$$

where $E = E_f - \varepsilon_n$. Here and below, the lower index 0 is omitted in the Green's functions and in the related quantities.

Due to the complex nature of $\mathcal{V}(E)$ the spectral representation of $\mathcal{G}(E)$ involves a biorthogonal expansion in terms of the eigenfunctions of $\mathcal{V}(E)$ and of its Hermitian conjugate $\mathcal{V}^\dagger(E)$. We consider the incoming wave scattering solutions of the eigenvalue equations, i.e.,

$$(\mathcal{E} - T - \mathcal{V}^\dagger(E)) | \chi_{\mathcal{E}}^{(-)}(E) \rangle = 0 , \quad (23)$$

$$(\mathcal{E} - T - \mathcal{V}(E)) | \tilde{\chi}_{\mathcal{E}}^{(-)}(E) \rangle = 0 . \quad (24)$$

The choice of incoming wave solutions is not strictly necessary, but it is convenient in order to have a closer comparison with the treatment of the exclusive $(e, e'N)$ reactions, where the final states fulfill this asymptotic condition and are the eigenfunctions $|\chi_E^{(-)}(E)\rangle$ of $\mathcal{V}^\dagger(E)$.

The eigenfunctions of Eqs. (23) and (24) satisfy the biorthogonality condition

$$\langle \chi_{\mathcal{E}}^{(-)}(E) | \tilde{\chi}_{\mathcal{E}'}^{(-)}(E) \rangle = \delta(\mathcal{E} - \mathcal{E}') , \quad (25)$$

and, in absence of bound eigenstates, the completeness relation

$$\int_M^\infty d\mathcal{E} |\tilde{\chi}_{\mathcal{E}}^{(-)}(E)\rangle \langle \chi_{\mathcal{E}}^{(-)}(E)| = 1 \quad (26)$$

where the nucleon mass M is the threshold of the continuum of the Feshbach Hamiltonian.

Eqs. (25) and (26) are the mathematical basis for the biorthogonal expansions. The contribution of possible bound state solutions of Eqs. (23) and (24) can be disregarded in Eq. (26) since their effect on the hadron tensor is negligible at the energy and momentum transfers considered in this paper.

Using Eqs. (26) and (24), one obtains the spectral representation

$$\mathcal{G}(E) = \int_M^\infty d\mathcal{E} |\tilde{\chi}_{\mathcal{E}}^{(-)}(E)\rangle \frac{1}{E - \mathcal{E} + i\eta} \langle \chi_{\mathcal{E}}^{(-)}(E) | . \quad (27)$$

Therefore, Eq. (22) can be written as

$$W^{\mu\mu}(\omega, q) = -\frac{1}{\pi} \sum_n \text{Im} \left[\int_M^\infty d\mathcal{E} \frac{1}{E_f - \varepsilon_n - \mathcal{E} + i\eta} T_n^{\mu\mu}(\mathcal{E}, E_f - \varepsilon_n) \right] , \quad (28)$$

where

$$\begin{aligned} T_n^{\mu\mu}(\mathcal{E}, E) &= \lambda_n \langle \varphi_n | j^{\mu\dagger}(\mathbf{q}) \sqrt{1 - \mathcal{V}'(E)} | \tilde{\chi}_{\mathcal{E}}^{(-)}(E) \rangle \\ &\times \langle \chi_{\mathcal{E}}^{(-)}(E) | \sqrt{1 - \mathcal{V}'(E)} j^\mu(\mathbf{q}) | \varphi_n \rangle . \end{aligned} \quad (29)$$

The limit for $\eta \rightarrow +0$, understood before the integral of Eq. (28), can be calculated exploiting the standard symbolic relation

$$\lim_{\eta \rightarrow 0} \frac{1}{E - \mathcal{E} + i\eta} = \mathcal{P} \left(\frac{1}{E - \mathcal{E}} \right) - i\pi \delta(E - \mathcal{E}) , \quad (30)$$

where \mathcal{P} denotes the principal value of the integral. Therefore, Eq. (28) reads

$$\begin{aligned} W^{\mu\mu}(\omega, q) &= \sum_n \left[\text{Re} T_n^{\mu\mu}(E_f - \varepsilon_n, E_f - \varepsilon_n) \right. \\ &\quad \left. - \frac{1}{\pi} \mathcal{P} \int_M^\infty d\mathcal{E} \frac{1}{E_f - \varepsilon_n - \mathcal{E}} \text{Im} T_n^{\mu\mu}(\mathcal{E}, E_f - \varepsilon_n) \right] , \end{aligned} \quad (31)$$

which separately involves the real and imaginary parts of $T_n^{\mu\mu}$.

Some remarks on Eqs. (29) and (31) are in order. Disregarding the square root correction due to interference effects, one observes that in Eq. (29) the second matrix element (with the inclusion of $\sqrt{\lambda_n}$) is the transition amplitude for the single nucleon knockout from a nucleus in the state $|\Psi_0\rangle$ leaving the residual nucleus in the state $|n\rangle$. The attenuation of its strength, mathematically due to the imaginary part of \mathcal{V}^\dagger , is related to the flux lost towards the channels different from n . In the inclusive response this attenuation must be compensated by a corresponding gain due to the flux lost, towards the channel n , by the other final states asymptotically originated by the channels different from n . In the description provided by the spectral representation of Eq. (31), the compensation is performed by the first matrix element in the right hand side of Eq. (29), where the imaginary part of \mathcal{V} has the effect of increasing the strength. Similar considerations can be made, on the purely mathematical ground, for the integral of Eq. (31), where the amplitudes involved in $T_n^{\mu\mu}$ have no evident physical meaning as $\mathcal{E} \neq E_f - \varepsilon_n$. We want to stress here that in the Green's function approach it is just the imaginary part of \mathcal{V} which accounts for the redistribution of the strength among different channels.

The matrix elements in Eq. (29) contain the mean field $\mathcal{V}(E)$ and its Hermitian conjugate $\mathcal{V}^\dagger(E)$, which are nonlocal operator with a possibly complicated matrix structure. Neither microscopic nor empirical calculations of $\mathcal{V}(E)$ are available. In contrast, phenomenological optical potentials are available. They are obtained from fits to experimental data, are local and involve scalar and vector components only. The necessary replacement of the mean field by the empirical optical model potential is, however, a delicate step.

In the nonrelativistic treatment of Refs. [11, 18] this replacement is justified on the basis of the approximated equation (holding for every state $|\psi\rangle$)

$$\begin{aligned} & \text{Im}\langle\psi | \sqrt{1 - \mathcal{V}'(E)}\mathcal{G}(E)\sqrt{1 - \mathcal{V}'(E)} | \psi\rangle \\ & \simeq \text{Im}\langle\psi | \sqrt{1 - \mathcal{V}'_L(E)}\mathcal{G}_L(E)\sqrt{1 - \mathcal{V}'_L(E)} | \psi\rangle, \end{aligned} \quad (32)$$

where $\mathcal{V}_L(E)$ is the local phase-equivalent potential identified with the phenomenological optical model potential and $\mathcal{G}_L(E)$ is the related Green's function. We have reasonable confidence that Eq. (32) holds also in the relativistic context.

3 Results

The response functions of the inclusive QE electron scattering are calculated from the single-particle expression of the coherent hadron tensor in Eq. (31). After the replacement of the mean field $\mathcal{V}(E)$ by the empirical optical model potential $\mathcal{V}_L(E)$, the matrix elements of the nuclear current operator in Eq. (29) are of the same kind as those giving the transition amplitudes of the electron induced nucleon knockout reaction in the distorted wave impulse approximation (DWIA) [1]. Thus, calculations have been performed adopting the same relativistic [20] and

nonrelativistic treatments [19] which were successfully applied to describe exclusive $(e, e'p)$ data, and with the same phenomenological ingredients for bound state wave functions and optical potentials.

In the calculations the residual nucleus states $|n\rangle$ are restricted to be single particle one-hole states in the target. A pure shell model is assumed for the nuclear structure, i.e., we take a unitary spectral strength for each single particle state and the sum runs over all the occupied states. In this way we are able to account for the contributions of all the nucleons in the nucleus, but correlations are completely neglected. This is of course an approximation that anyhow allows us to perform relatively simple calculations on a conceptually clear basis.

The hadron tensor in Eq. (31) is the sum of two terms. The calculation of the second term, which requires integration over all the eigenfunctions of the continuum spectrum of the optical potential, is a rather complicate task. The contribution of this term is very small and can be neglected in the nonrelativistic frame [11], while in the relativistic frame it can be significant and must included in the calculation [13].

The longitudinal and transverse response functions calculated in the relativistic frame for ^{12}C at $q = 400 \text{ MeV}/c$ are displayed in Fig. 1 and compared with the Saclay data [21]. The low energy transfer values are not given because the relativistic optical potentials are not available at low energies.

The agreement with the data is generally satisfactory for the R_L . In contrast, R_T is underestimated. This is a systematic result of both relativistic and nonrelativistic calculations. It may be attributed to physical effects which are not considered in the present approach, e.g., two-body currents. The effect of the integral in Eq. (31) is also displayed. At variance with the nonrelativistic result [11], this contribution is important and essential to reproduce the experimental longitudinal response. The contribution of interference between different channels, that produces the factor $\sqrt{1 - \mathcal{V}'_L(E)}$, gives only a negligible contribution in Fig. 1, while in the nonrelativistic calculation this contribution is important to improve the agreement with R_L data [11].

The contribution from all the integrated single nucleon knockout channels is also drawn in Fig. 1. It is significantly smaller than the complete calculation. The reduction, which is larger at lower values of ω , gives an indication of the relevance of inelastic channels.

An example of the comparison between the results of the relativistic and the nonrelativistic approaches is presented in Fig. 2 for the longitudinal response at $q = 400 \text{ MeV}/c$. Both complete calculations are in satisfactory agreement with the data. This result is however due to a different effect of the various contributions in the two approaches. In the nonrelativistic case the factor $\sqrt{1 - \mathcal{V}'_L(E)}$ produces a substantial reduction of the calculated response, that is necessary to reproduce the data. The integral in the second term of Eq. (31) gives only a small contribution and is neglected in the calculation. In the relativistic approach the integral is essential to reproduce the data while the interference between different channels is generally negligible.

The longitudinal and transverse response functions calculated in the relativistic approach for ^{12}C at $q = 500$ are displayed in Fig. 3 and compared with the Saclay data [21]. As already found in Fig. 1 at $q = 400$ MeV/ c , a good agreement with the data is obtained for R_L , while R_T is underestimated. Also in Fig. 3 only a slight effect is given by the interference between different channels. The role of the integral in Eq. (31) decreases increasing the momentum transfer. The effect of the inelastic channels, indicated in the figure by the difference between the complete results and the contribution from all the integrated single nucleon knockout channels, is always visible and even sizable, but it decreases increasing the momentum transfer.

The response functions for ^{40}Ca at $q = 450$ MeV/ c are shown in Fig. 4 and compared with the available data. The calculated results are of the same order of magnitude as the MIT-Bates data, while for the Saclay data R_L is overestimated and R_T underestimated. The factor $\sqrt{1 - \mathcal{V}'_L(E)}$ produces an enhancement which is minimal but visible in the figure.

4 Conclusions

A Green's function approach to inclusive QE electron scattering has been presented. The components of the hadron tensor are written in terms of Green's functions of the optical potentials related to the various reaction channels. The projection operator formalism is used to derive this result. An explicit calculation of the single-particle Green's function can be avoided by means of its spectral representation, based on a biorthogonal expansion in terms of the eigenfunctions of the non-Hermitian optical potential $\mathcal{V}(E)$ and of its Hermitian conjugate. The interference between different channels is taken into account by the factor $\sqrt{1 - \mathcal{V}'(E)}$, which also allows the replacement of the mean field $\mathcal{V}(E)$ by the phenomenological optical potential $\mathcal{V}_L(E)$. After this replacement, the nuclear response functions are expressed in terms of matrix elements similar to the ones which appear in the exclusive one nucleon knockout reactions, and the same DWIA treatment can be applied to the calculation of the inclusive electron scattering.

The effects of FSI are thus described consistently in exclusive and inclusive processes. Both the real and imaginary parts of the optical potential must be included. In the exclusive reaction the imaginary part accounts for the flux lost towards other final states. In the inclusive reaction, where all the final states are included, the imaginary part accounts for the redistribution of the strength among the different channels.

All the final states contributing to the inclusive reaction are contained in the Green's function, and not only one nucleon emission. Our calculations for the inclusive electron scattering are different from the contribution of integrated single nucleon knockout only. The difference between the two results is originated by the imaginary part of the optical potential.

FSI effects are similar on the longitudinal and transverse components of the nuclear response and are important both in the relativistic and in the nonrelativistic

calculations. The role and relevance of the various effects can however be different in the two frames. The final effect is similar and produces qualitatively similar results in comparison with data. The longitudinal response is usually well reproduced, while the transverse response is underestimated. This seems to indicate that more complicated effects, e.g., two-body meson exchange currents, have to be added to the present single particle approach.

References

- [1] S. Boffi, C. Giusti and F.D. Pacati, Phys. Rep. **226**, 1 (1993);
S. Boffi, C. Giusti, F.D. Pacati and M. Radici, *Electromagnetic Response of Atomic Nuclei* (Clarendon Press, Oxford, 1996).
- [2] E.J. Moniz *et al.*, Phys. Rev. Lett. **26**, 445 (1971).
- [3] M.N. Rosenbluth, Phys. Rev. **79**, 615 (1950).
- [4] J.P. Chen, S. Choi, and Z.E. Meziani, spokespersons, JLab experiment E-01-016.
- [5] I. Sick, in *Nuclear Theory*, (Heron Press Science Series, Sofia, 2002), p. 16.
- [6] W. Leidemann and G. Orlandini, Nucl. Phys. **A506**, 447 (1990)
- [7] A. Fabrocini, Phys. Rev. C **55**, 338 (1997)
- [8] Y. Horikawa, F. Lenz, and N.C. Mukhopadhyay, Phys. Rev. C **22**, 1680 (1980).
- [9] C.R. Chinn, A. Picklesimer, and J.W. Van Orden, Phys. Rev. C **40**, 790 (1989); Phys. Rev. C **40**, 1159 (1989).
- [10] P.M. Boucher and J.W. Van Orden, Phys. Rev. C **43**, 582 (1991).
- [11] F. Capuzzi, C. Giusti, and F.D. Pacati, Nucl. Phys. **A524**, 681 (1991).
- [12] F. Capuzzi and C. Mahaux, Ann. Phys. (N.Y.) **254**, 130 (1997).
- [13] A. Meucci, F. Capuzzi, C. Giusti, and F.D. Pacati, Phys. Rev. C **67**, 054601 (2003).
- [14] G.B. West, Phys. Rep. **18**, 264 (1975).
- [15] G. Orlandini and M. Traini, Rept. Prog. Phys. **54**, 257 (1991).
- [16] S. Boffi and F. Capuzzi, Nucl. Phys. **A351**, 219 (1981).
- [17] H. Feshbach, Ann. Phys. (N.Y.) **5**, 357 (1958).
- [18] F. Capuzzi, Nucl. Phys. **A554**, 362 (1993).

- [19] C. Giusti and F.D. Pacati, Nucl. Phys. **A473**, 717 (1987); Nucl. Phys. **A485**, 461 (1988).
- [20] A. Meucci, C. Giusti, and F. D. Pacati, Phys. Rev. C **64**, 014604 (2001).
- [21] P. Barreau *et al.*, Nucl. Phys. **A402**, 515 (1983); Note CEA N-2334.
- [22] Z.E. Meziani *et al.*, Phys. Rev. Lett. **52**, 2130 (1984); **54**, 1233 (1985).
- [23] C.F. Williamson *et al.*, Phys. Rev. C **56**, 3152 (1997).

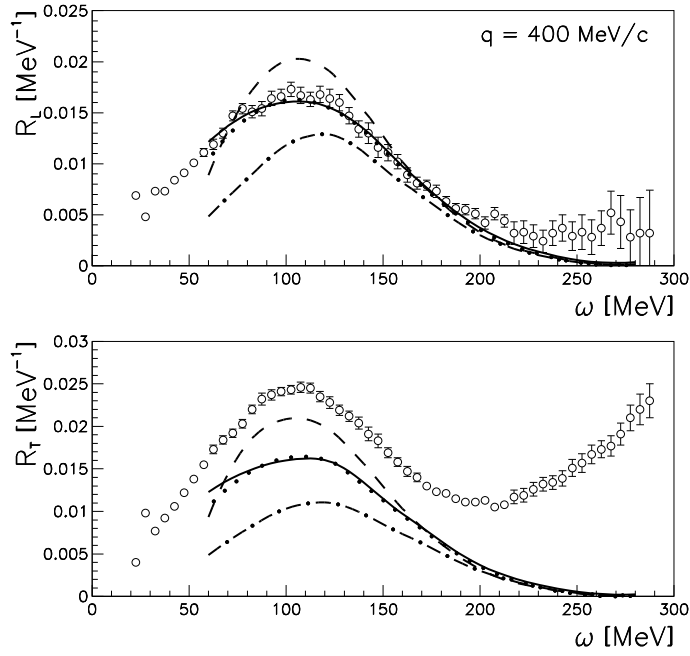


Figure 1: Longitudinal (upper panel) and transverse (lower panel) response functions for the $^{12}\text{C}(e, e')$ reaction at $q = 400 \text{ MeV}/c$ calculated in the relativistic frame. Solid and dotted lines are obtained with and without the factor $\sqrt{1 - \mathcal{V}'(E)}$, respectively. Dashed lines give the result without the integral in Eq. (31). Dot-dashed lines are the contribution of integrated single nucleon knockout only. The data are from Ref. [21]. (from Ref. [13])

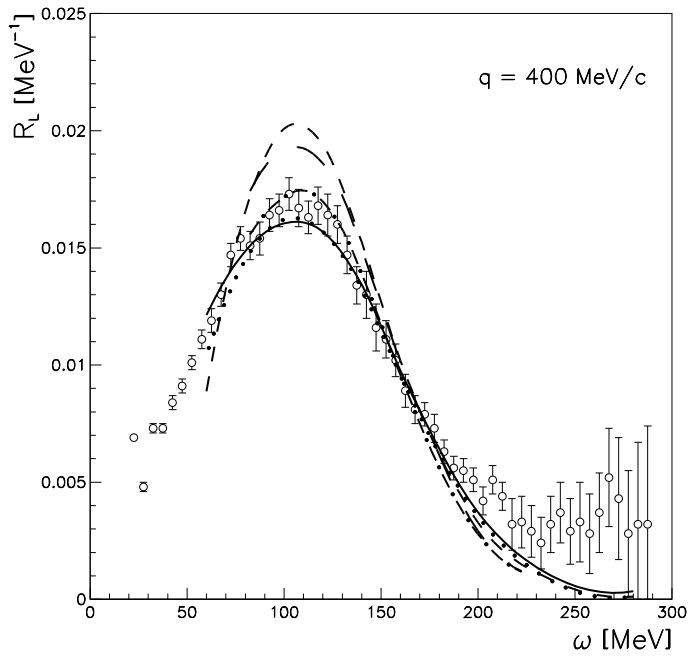


Figure 2: Longitudinal response function for the $^{12}\text{C}(e, e')$ reaction at $q = 400$ MeV/ c . Solid dotted and dashed lines are the same as in the upper panel of Fig. 1. Dot-dashed and long-dashed lines are the nonrelativistic results with and without the factor $\sqrt{1 - \mathcal{V}'(E)}$, respectively. Data as in Fig.1. (from Ref. [13])

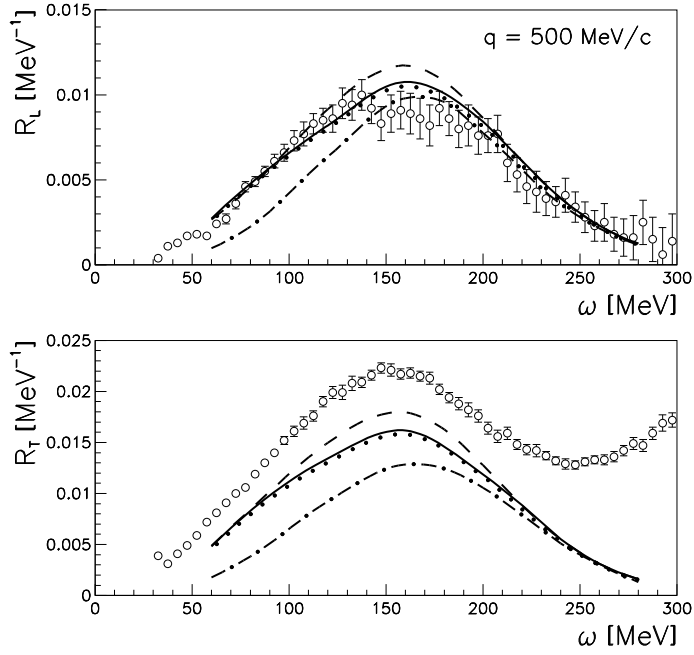


Figure 3: The same as in Fig. 1, but for $q = 500$ MeV/ c . The data are from Ref. [21]. (from Ref. [13])

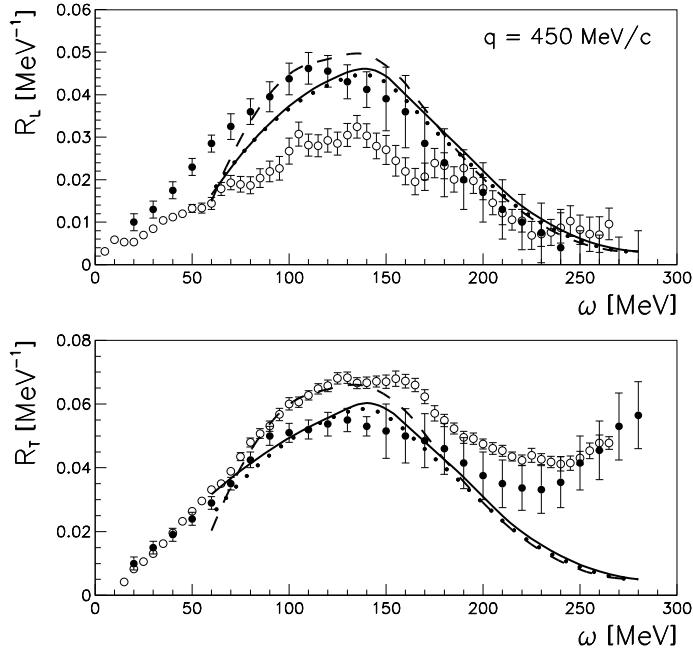


Figure 4: Longitudinal (upper panel) and transverse (lower panel) response functions for the $^{40}\text{Ca}(e, e')$ reaction at $q = 450 \text{ MeV}/c$. The Saclay data (open circles) are from Ref. [22], the MIT-Bates (black circles) are from Ref. [23]. Line convention as in Fig. 1. (from Ref. [13])